MODELLING, OPERATION AND CONTROL OF MULTITERMINAL DC CONNECTION FOR OFFSHORE WIND FARMS

**Mircea Viorel DRAGAN, Cristina Madalina DRAGAN,
Crina Violeta DRAGAN, Doru HANGANU**
"Dunărea de Jos" University of Galati
email: vdragan@ugal.ro

ABSTRACT

Renewable energy systems are tending to become more and more present in the energy market and wind power has already proven its potential. Wind parks of thousands of MW are planned to be place into sea faraway from the mainland. Appropriate transmission systems should be designed in order to be able to handle a significant amount of power with high efficiency and to be economically competitive. This paper discusses a Multiterminal DC connection, based on VSC technology, between one offshore wind farm and two different grids. The main focus was on developing the control strategy for connecting these three systems via DC connection. The modelling and designing of the WF components, of the power converters, of the DC system components and of all the controllers played a major role in developing a simulation platform for future studies. The proposed concept may enable integration of large offshore wind farms at considerable distances. Experimental verifications follow the theoretical investigations in order to prove the reability of the modelled system for different test scenarios.

KEYWORDS: multiterminal DC power wind farm, modelling, simulation, Power Factory DIgSILENT

1. Introduction

Offshore wind energy is one of the key component in helping the EU to fulfil the agreement to achieve the 20% of renewable energy from the total energy by 2020.

Although the offshore market is currently smaller then the onshore one, it is of high interest for the energy policies because of its important capacity of producing energy.

The offshore wind market is characterized by projects that are significantly larger and more difficult to implement than most of the onshore projects [1]. Currently limitations are encountered in connecting the large scale offshore wind energy.

Also the current onshore transmission networks can not be able to integrate the energy that can be available in most of the large scale offshore projects.

To correct these deficiencies a redesign of the grid infrastructure, system management, grid regulation and grid codes are needed.

The large scale offshore wind farms have to be treated as conventional power plants, thus the necessity for both national and cross border network upgrades is increasing.

2. Transmission features for offshore Wind farms

One of the challenges is to find a suitable type of connection for offshore wind farms, having different power ratings and different distances from the onshore connection point. This selection should be done by taking into consideration power efficiency and economical aspects. Until now for the already build WFs, like Horns Rev I, Nysted, Middelgrunden, in Denmark, the only connection used was the AC connection. The reasons for choosing this type are: lower station costs, no power converters needed, a simple layout for the offshore park. By choosing the AC transmission for the offshore WF several disadvantages are encountered, such as: the need of reactive power compensators, such as SVCs or STATCOMs, AC cable cost becomes higher as the distance grows, the decrease of the transmission capability of AC system decreases together with distance because of the dielectric losses and the reactive power that is produced along the cable.

The solution could be the HVDC transmission. Some benefits of using HVDC transmission instead of AC transmission are: less power losses for long

distances, lower cost for cables above certain distances, connection of asynchronous AC networks and offshore WFs can operate at variable speeds.

When it comes to decide which is the best transmission system option, two parameters which have a great impact on transmission efficiency and costs are considered. These are the transmitted power and the distance. Figure 1 reveals what is the suitable connection type for electrical systems.
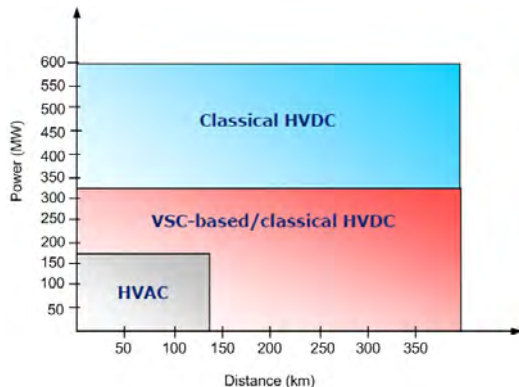

Fig 1.Transmission type depending on power and distance [2]

It can be seen that the HVAC is the best solution for small power systems and short distances. One of the reason is the increased price for installations and cables when it comes to transmit high levels of power on long distances. As the power and distances increase the HVDC connection should be considered. The VSC-HVDC technology is preferable to transmit medium amount of power on long distances, but when it comes to transmit on large distances a significant amount of power, the solution is classic HVDC.

The HVDC-VSC transmission is a relatively new technology that uses the latest power semiconductor, the IGBTs.

These power semiconductors have self-commuted turn-on and turn-off capability, thus allow generating reactive power to supply wind turbines in the offshore station while active power injected to the transmission system can be control. With the development of this semiconductor and control equipment, the voltage source converter became viable systems. The HVDCVSC technology is used by several manufacturers, two of them can be mentioned: Siemens which developed HVDC Plus (12 pulses) and ABB which HVDC Light (6 pulses).

The advantages provided by using HVDC-VSC in an wind farm are:
- Smaller transformer substations;
- Low weight DC cables making the process easier to transport, install and more economical;
- Ensures reactive power compensation;
- It can be easily expanded;
- Fault ride-through and black start capability.

Currently one of the concerns is the limited power exchange between the EU country members due to the lack of physical interconnection capacity and the capacity allocation mechanisms.

The development of the offshore wind farms is one of the factors that leads to the demand of increased interconnections and improve the possibility of power exchange.

Taking into consideration the advantages of the HVDC-VSC technology, the suitable solution that can provide the offshore WFs connection and also that can facilitate the trans-national exchange with a high cost efficiency, is the multiterminal DC transmission system (MTDC).

3. Modelling

A number of three identical wind turbines connected in parallel are modelled for the wind farm configuration. The generating side of each WT is connected with the AC/DC side of a full scale power converter, through a phase reactor in parallel with an AC filter. Each wind turbine was designed to have its own rectifier. The output power of the wind farm is linked in a common point offshore, followed by a step up DC/DC booster. Next two DC links will connect each grid. An inverter is placed on both of the grid sides. The main function of the VSC-HVDC is to transmit constant DC power from the rectifiers to the inverters. The connection to the grids is made through a set of phase reactors and AC filters. A transformer is also used for AC voltage boosting and galvanic isolation.

The modelling includes a wind turbine system, a wind turbine full scale power converters control, and a grid side converters control.

3.1. Wind Turbine Model
The wind turbine's rotor extracts the kinetic power from the wind and transforms it into mechanical power. Then the mechanical power is converted into electrical energy by the generator and fed into the grids through converters. A simplified block diagram of the wind turbine components is presented in Figure 2. As shown in the scheme, the elements of wind turbine are the wind model, the aerodynamic model, the mechanical model, the generator model, the rectifier and the pitch control block model.
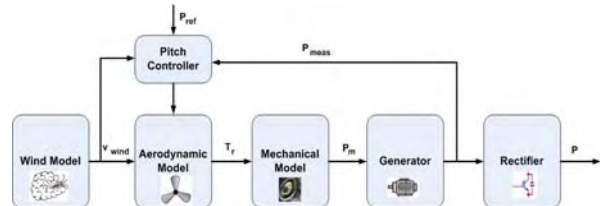

Fig. 2. Layout of the Wind Turbine Model

The input of the system is the wind and the output is the electrical power. The wind model provides a realistic characteristic of the wind which is modelled based on an average wind speed profile. This wind is further on applied to the rotor blades. The aerodynamic model computes the rotor torque (T_r) which is the input for the mechanical model that makes the conversion of the mechanical torque of rotor into a torque proper for the high speed shaft. For the generator model a squirrel cage induction generator is used. This performs the conversion of the mechanical power outputted by the mechanical model (P_m) into the electrical power (P_{meas}), followed by the transformation from an AC to DC transmission system made by the rectifier.

The aim of the pitch controller is to ensure that the wind turbine, depending on the available wind is producing the desired power imposed by the TSO. Based on the measured power of the system and the reference value for power, the pitch control has to adjust the angle of the blades in order

to maintain a constant reference power when higher winds are applied to the WT. The power reference can be set to be the rated power of the WT but depending on the demands of electricity. The grid operator can change this reference in order to maintain the stability of the grid. The offshore wind farm represents the third terminal in the MTDC system.

3.2. Generator Side Converter

The main issue regarding the control of the full power scale converter (sending end station) for the wind turbine is to ensure system stability and maximum operating point of the generators by providing suitable voltage and frequency set-points on to the grid. For optimizing the power output of the SCIGs, the constant voltage/frequency control has been implemented for the generator side converters.

Each wind turbine is equipped with a 2,3 MW squirrel cage induction generator. Figure 3 shows the generator's power output having the pitch angle set to its optimal value and having a wind speed that varies from the cut-in wind speed (4m/s) to the rated wind speed (11.9m/s). Even if the pitch angle is equal to the optimal value, the operating points of the active power are not optimal due to low wind speeds. Figure 3 indicates that the rated active power is achieved for the rated synchronous speed that corresponds to the frequency of 50 Hz. Therefore, for wind speeds below the rated values, the optimum operational points of the WT must be found. This is done by varying the generator's synchronous speed. The interval of variation for the synchronous speed is considered between 500 and 1500 rpm. The black line drawn in Figure 3 shows these points. The range of speed operation is obtained for a maximum output of the

WT for all the considered wind speeds [3]. Considering Figure 3 the optimal frequency for the stator side of the SCIG for different wind speed is computed.
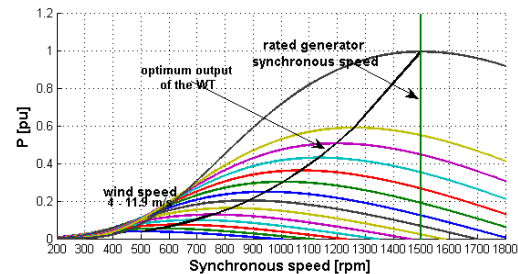

Fig. 3. *Power output of the generators for different wind speeds*

The control scheme of the rectifiers implemented in Power Factory is based on the dependence of frequency on active power and voltage on reactive power from Figure 4.
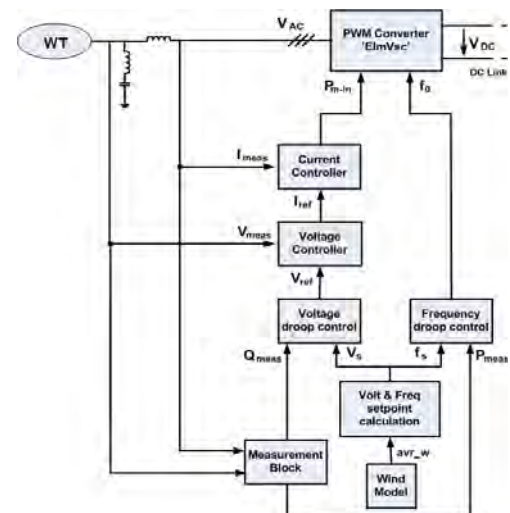

Fig. 4. *Control structure of the rectifiers*

As depicted Figure 4 the control of the rectifier is composed of voltage-frequency control, frequency droop control block, voltage droop control block and PI regulators for voltage and current. Using the Pulse Width Modulation (PWM) technique in the VSC converter, it is possible to obtain the desired voltage waveform at the AC terminals. Limitations apply due to the power ratings of the converter, the DC voltage and the maximum switching frequency. The inputs of the PWM model are P_{min-in} and f_0 and they can be adjusted independently by the VSC converter to give any combination of voltage magnitude and phase shift in relation to the fundamental frequency-voltage in the WT side. A measurement block is used to obtain information about the AC current and voltage on the AC side. These signals are used for the current and

voltage loops in order to minimize the errors. I_{meas} and V_{meas} are also used to calculate the active and reactive power on the AC side. So, according to the V/f constant principle the optimal output voltage can be calculate according to (1):

$$\frac{Vrated}{frated} = ct \qquad (1)$$

Therefore by keeping the ratio between voltage and frequency constant, the voltage set-point Vs is obtained. :

$$\frac{Vs}{fs} = \frac{Vrated}{frated} \qquad (2)$$

The setpoints for frequency and voltage provided by the Voltage and Frequency setpoint calculation block are optimized by the *Voltage droop* control and *Frequency droop* control blocks.

The voltage control loop should ensure that the reactive currents, which circulate inside the wind farm, are within limits. A droop characteristic for the voltage controller will minimize the stationary error in this case. Since the induction generator will always draw reactive power from the PWM converter, the voltage reference should be increased when the generator's demand for reactive power increases [4]. Voltage reference for the voltage controller is calculated using Eq. 4.

In order to optimize the transfer of the entire available power from the wind farm to the main power grid, a frequency droop characteristic is used. The set-point frequency provided by the V/f block is optimized as a function of the produced power as shown in Eq. 3.

$$V_{ref} = V_s + K_v \cdot Q_{meas} \qquad (3)$$

$$f_0 = f_s - K_f(1 - P_{meas}) \qquad (4)$$

where: K_f - frequency droop coefficient, $K_f = \frac{\Delta f}{\Delta p}$; K_v - voltage droop coefficient; V_s - voltage setpoint fed by the V/f control system.

3.3. Grid Side Converter

While the converters connected to each wind turbine control the active power flow and the AC voltage, the receiving end stations are designed to control the DC link voltage and the reactive power. For the grid connected applications, the typical control strategy of the VSC-HVDC receiving end station is the voltage oriented control.
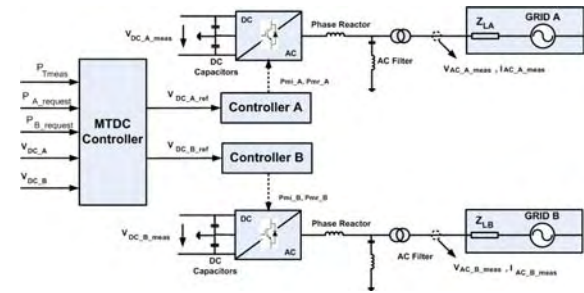

Fig. 5. *Overall control structure of the receiving end stations implied in MTDC [3]*

The overall control structure of the receiving end stations of System A and System B is presented in Figure 5. It is based on the linear dependence of the DC voltage on the active power. The control block implemented in DIgSILENT Power Factory contains the MTDC Controller that handles with the active power sharing between the two grids, function of the measured output of the wind farm PTmeas, the power demands of each grid (P1 for GRID A and P2 for GRID B) and the DC voltage levels from each inverter. Communication lines are needed between the three terminals for real time acquisition of the terminals parameters. The MTDC Controller takes into consideration also the losses from the transmission system that is represented by intern parameters. For a more accurate computation, the losses have to be monitored in real time.
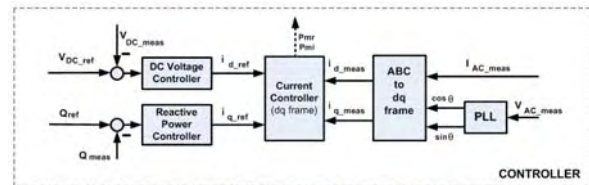

Fig. 6. *Detailed control structure of receiving end converter [3]*

Based on these parameters, the MTDC Controller block supplies the DC voltage setpoints for both of the controllers for GRID A and GRID B. The control blocks for each inverter are identical and a detailed structure is shown in Figure 6. The main control blocks contain a fast current controller that outputs the real and imaginary part of the modulation index. The references values for the current controller block are provided by additional controllers for the DC voltage and reactive power.

The reference for the 'Reactive Power Controller' are given by each TSO of GRID A and GRID B. The setpoints for the DC voltage controller are sent by the MTDC controller for each inverter. The measuring points of DC voltage, AC voltage and AC current are placed in each of the system as indicated in Figure 5. A PLL block is used in order to

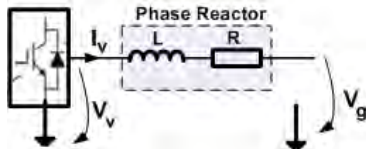synchronize the phase of the dq references with the AC source voltage.

Fig. 7. *Equivalent circuit of the receiving end station*

The equivalent circuit of a single phase receiving end converter is shown in Figure 7 where the converter and the grid can be considered as voltage sources V_v and V_g. It is considered that the circuit is functioning at the nominal frequency 50 Hz, thus the AC filter can be neglected [4].

Looking at the circuit from Figure 7, the voltage on the phase reactor can be derived as:

$$V_v - V_g = L\frac{div}{dt} + Ri_v, \quad (5)$$
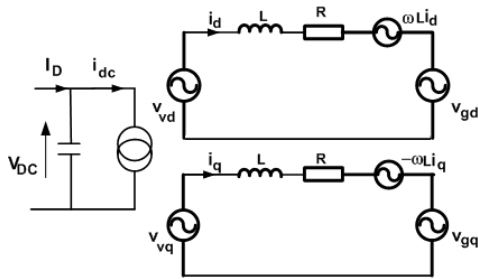
Fig. 8. *VSC equivalent circuit in dq reference frame*

In order to decouple the DC voltage and the reactive power controllers, the synchronous rotation dq reference frame is used.

First (5) is translated from the abc stationary frame in the $\alpha\beta$ orthogonal coordinates using the Clarke Transform.

The voltage droop on the line reactor in $\alpha\beta$ coordinates is [5]:

$$\begin{cases} V_{v\alpha} - V_{g\beta} = L\dfrac{di_{v\alpha}}{dt} + Ri_{v\alpha} \\ \\ V_{v\beta} - V_{g\beta} = L\dfrac{di_{v\beta}}{dt} + Ri_{v\beta} \end{cases} \quad (6)$$

where the voltages Vv and Vg have the following expression in $\alpha\beta$ stationary frame function of the abc coordinates:

$$V_\alpha = \sqrt{3} \cdot V_{ab} + \frac{\sqrt{3}}{2}V_{bc} \quad (7)$$

$$V_\beta = \frac{3}{2}V_{bc} \quad (8)$$

Furthermore, using the Park transformation Eq. (6) are expressed in the dq coordinates:

$$\begin{cases} V_{vd} - V_{gd} = L\dfrac{di_{vd}}{dt} + j\omega Li_{vq} + Ri_{vd} \\ \\ V_{vq} - V_{gq} = L\dfrac{di_{vq}}{dt} + j\omega Li_{vd} + Ri_{vq} \end{cases} \quad (9)$$

The relation between the dq and $\alpha\beta$ quantities is [6]:

$$\begin{cases} V_d = \dfrac{2}{3\sqrt{2}}(V_\alpha \cos\theta - V_\beta \sin\theta) \\ \\ V_q = \dfrac{2}{3\sqrt{2}}(V_\beta \cos\theta + V_\alpha \sin\theta) \end{cases} \quad (10)$$

where: θ – the angle between the α and β axes:

$$\theta = \arctan\frac{V_\beta}{V_\alpha};$$

ω - the angular frequency: $\omega = \dfrac{d\theta}{dt}$;

Based on (9) the VSC equivalent circuit is obtained in the dq axes representation as shown in Figure 8.

By assuming that the d-axis is aligned with the axis of one phase voltage V_v from stationary abc reference frame, it results that $V_{vq} = 0$ and $V_{vd} = V_v$ [6]. From Figure 8, the apparent power injected by the converter in the AC grid can be written as [7]:

$$S = 3(V_{vd} + j0)(i_d - ji_q) \quad (11)$$

Therefore, the active and reactive powers are:

$$P_{DC} = P_{AC} = 3V_{vd}i_d \quad (12)$$

$$Q = -3V_{vd}i_q \quad (13)$$

It can be observed that the active power is related to the current id and the reactive power to iq. Relation (12) must be satisfied in order to ensure the stability of the system. Any unbalance in the active power flow transferred through the converter will cause DC voltage fluctuations. Therefore, to provide reference values for the currents id and I which are responsible for controlling the DC voltage and reactive power control loops must be used.

Equation (12) can be written as:

$$V_{DC}i_{dc} = 3V_{vd}i_d \quad (14)$$

The real part of the modulation index of the inverter corresponding to the d axis is [9]:

$$P_{mr} = \frac{v_{gd} 2\sqrt{2}}{V_{DC}} \qquad (15)$$

From (14) and (15) the relation between the current of the d axes and the DC current is:

$$i_{dc} = \frac{3}{2\sqrt{2}} P_m i_d \qquad (16)$$

The variation of the DC voltage is given by the voltage droop VD on the capacitor from the DC side of the converter:

$$\frac{dV_{DC}}{dt} = \frac{1}{C}(I_D - i_{dc}) \qquad (17)$$

If it is assumed that the DC voltage is constant, the voltage on the capacitor is zero and $I_D = i_{dc}$.

By using this assumption in (16) and (17) the DC voltage can be written as:

$$V_{DC} = \frac{1}{C}\int (I_D - \frac{3P_m i_d}{2\sqrt{2}})dt \quad (18)$$
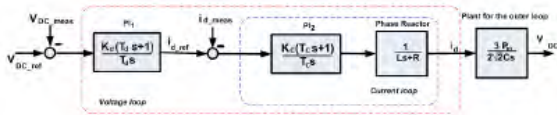
Fig. 9. *Outer loop and inner loop controllers of the receiving end station*

The fast current controllers used for obtaining the id and iq currents are complemented with additionally controllers that output the reference values needed for the voltage controller and reactive power. Therefore the current controllers represent the inner controller and the outer controllers are the DC voltage and reactive power controllers. The control scheme for the DC voltage is described in Figure 9. The control loops for d and q axes are the same, resulting in design of identical PIs for each loop.

4. Simulation results

Different study cases were performed in order to verify and illustrate the performance of the control system for the entire structure of a small offshore wind farm connected to a HVDC line transmission system.

4.1. Study Case 1 - Voltage/Hertz Controller

The purpose of this simulation is to test the efficiency of the voltage/frequency controller implemented for the generator side converters.
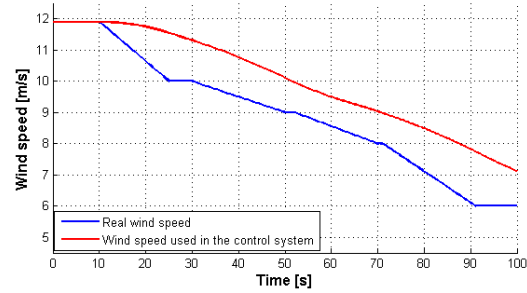

Fig. 10. *Wind profile for V/F controller*

The wind profile applied for this study case may be seen in Figure 10. For testing the controller, the averaged wind speed is computed by a moving average filter (green signal).

The moving average function is used to smooth out short term fluctuations. Having set the wind speed, two tests are made for analyzing the power generation: with and without V/f control

When the wind speed starts to have values below 11,9m/s, the frequency is adjusted in order to maximize the WT's power output.

Figure 11 presents the active power production of the induction generator. In blue is presented the power outputted by the WT without enabling the V/f control algorithm on the generator side converter. By activating the controller, the generation of active power (in red) is maximized by modifying the voltage and frequency setpoints.
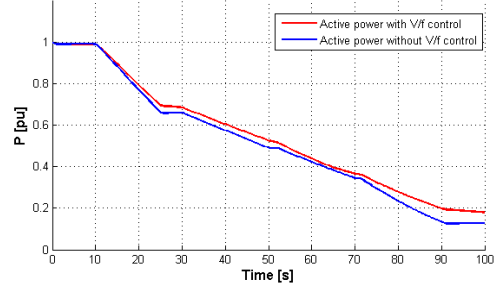

Fig.11. *Generator's active power with and without V/F control*

Comparing the results shown in Figure 11 it can be concluded that the power production with V/f control is higher than without it.

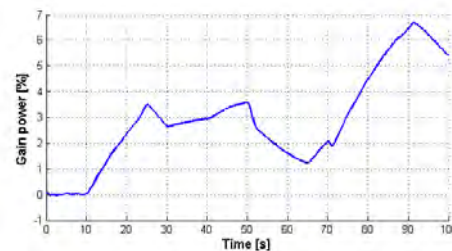From Figure 11 the gain in active power can be obtained.

Fig. 12. *Active power gain*

In the first time interval when the wind is kept constant to the rated value, the gain is zero because no control is active. When the wind speed drops the V/f controller starts actuating. Figure 12 highlights the gain in the power production by activating the voltage/frequency control for wind speeds within the interval [v_{cut-in}; v_{rated}].

The generator side converter proved its use in operation control for different wind speeds situations.

4.2. Study Case 2 - Pitch Controller

To test that the wind farm operates correctly, the power production of the WTs is analyzed. After designing the parameters of the PI for the pitch controller loop, the WF must be able to limit the power output as the wind speed increases over the rated value. The testing will be made using the real wind profile provided by the wind model of each WT. The simulations are run for 100 seconds.
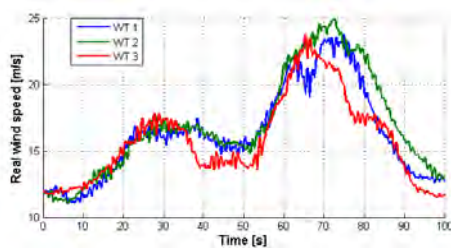

Fig 13. Wind speed profile

The average wind speeds vary from the rated value 11,9m/s until they reach 23m/s. Based on the average wind, the wind profiles outputted by the wind model are obtained. They are depicted in Figure 13. It can be seen that the three winds start to rise until they reach 23m/s and then drop to the rated value.
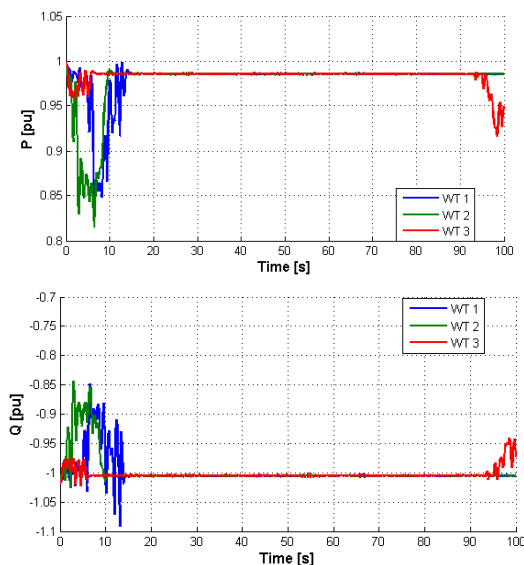

Fig. 14. Active and reactive power regulation

By activating the pitch control, the blades start to be pitched in and out of the wind in order to keep constant the power.

The pitch angle variations should be directly proportional with the wind.

In the first time interval the wind speed is at the rated value, the pitch controller is inactive - thus, the pitch angle is maintained to zero in order to obtain the rated power value.

When the wind becomes greater than v_{rated}, the blade control angle is varying in such a way that it holds the powers to the nominal value (see Figure 14).

As it can be observed the active and reactive power limitation is achieved.

4.3. Study Case 3-Active Power Sharing

This study case deals with the analysis of the power sharing between the two grids. The simulations are based on the control algorithm investigated in [3]. The simulation conditions are:

- One WF and two grids situated at different distances are connected through the MTDC (GRID A 10 km from the offshore WF and GRID B 30 km from the offshore WF);

- The wind farm is functioning at the rated parameters.

Some simulations are performed with constant output power from the wind farm in order to analyze the DC voltage level fluctuations of the inverters of each of the grids depending on their power demands. Another set of simulations are made with a variable output power from the WF, to present a realistic behaviour of the MTDC system where the power generated by the WF is varying function of the wind speed.

- For all the simulations is considered that GRID A TSO settles the active power request. GRID B is adjusting its power consumption function of GRID A, meaning that is taking the excess of power from the WF or it is generating extra power for the GRID A in order for the active power demand to be accomplished. Figure 15 shows the active power request of GRID A that was considered. In all the simulation time the active power request varies from 100% to 10% from the total active power generated by the WF.
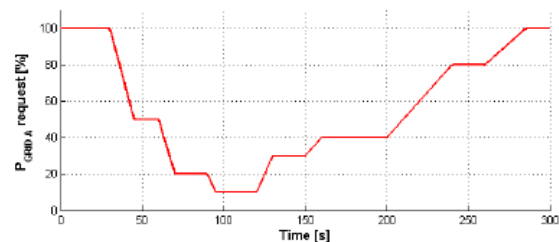

Fig. 15. Active power request from GRID A TSO

First it is considered the functioning of the wind turbines at nominal parameters and at constant wind speed conditions.

Thus the WF output active power is kept constant to its rated value of 0.8 pu.

Two cases were taking into account function of the two grids:

1. GRID A and GRID B are identical;

2. GRID B is stronger than GRID A having the short circuit power ten times greater;

By sending the power demand of GRID A shown in Figure 15 to the MTDC controller, the DC voltage reference points VDCA and VDCB of the grid side inverters are set. Both DC voltage levels follow an inverse proportionality dependence according to the active power consumptions as presented in Figure 16. Also the variation in DC voltage is proportional with the distance between the WF and the receiving end.
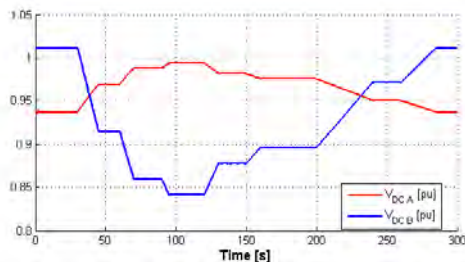

Fig. 16. *DC voltage set points for Converter$_{GRIDA}$ and Converter$_{GRIDB}$*

Converter$_{GRIDA}$ which is closer to the WF's PCC has smaller variations comparing to Converter$_{GRIDB}$. The DC voltage level has to be maintained in _5% limits of the rated value [10]. The maximum deviation of the DC voltage from the acceptable limit is recorded when GRID A demands only 10% of the total power. MTDC controller is sending to Converter$_{GRIDB}$ a reference value for the DC voltage that is lower than the the allowed limit, in order to fulfil the power sharing.

Therefore an additional control method has to be implemented in order to maintain the variations of the DC voltages in the allowed limits. One of the solution would be for the MTDC controller to be able to vary the DC voltage in the PCC of the WF in order to obtain smaller variations at the inverters terminals.
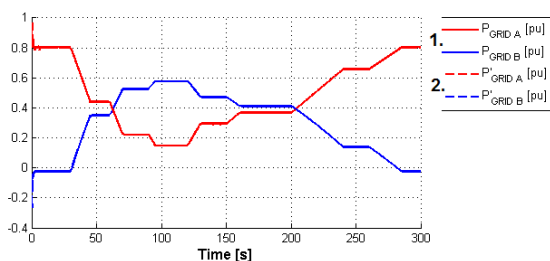

Fig.17. *Active power sharing between GRID A and GRID B in Case 1 and Case 2*

By knowing the DC voltage setpoints according to the power request of GRID A, the power sharing that was obtained between the two grids is shown in Figure 17. The power injected into the networks has the same variation in both cases.

Also no notifiable change exist between the two cases when the short circuit power of the grids is different.

The power sharing for GRID A follows the active power request from Figure 15. A small error exists between the imposed value for requested power and the one that is obtained as shown in 18 for GRID A. The maximum error is 6.5% and it occurs for the smallest power demand 10%. By looking at the error for all the MTDC system in Figure (b), the error is 11% for the same 10% value of power request from GRID A.
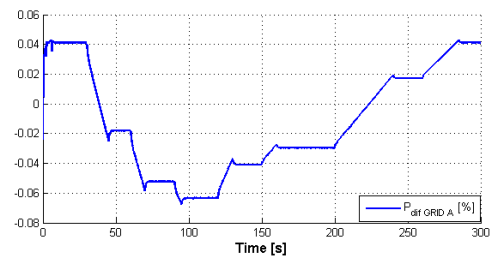
(a)
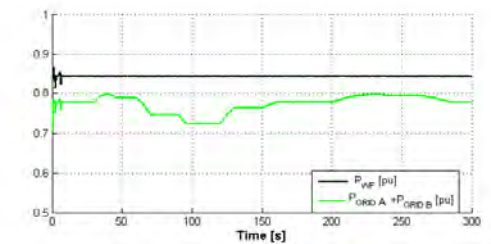
(b)

Fig. 18. *Power sharing error for (a) GRID A and (b) MTDC system*

These errors can be justified by the losses that exist in the system besides the losses from the DC cables. This difference in power is due to the power losses on the phase reactors and converters. For the power sharing algorithm based on steady state analysis only the losses of the DC cables were taken into consideration.
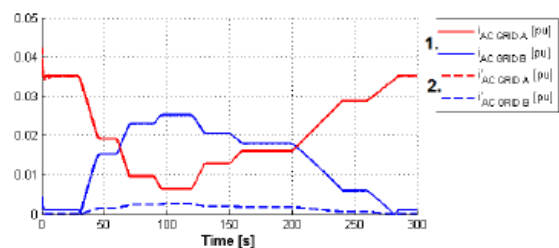

Fig. 19. *Current injected in GRID A and GRID B*

The different values of short circuit power influence the current injected into to grid and also the voltage and frequency in the PCC. Figure 19 presents the variation of currents injected in GRID A and GRID B for both cases, when the grids have the same short circuit power and when they don't

have the same short circuit power. The currents curves have the same shape as the active power flowing into the grids. It can be also observed that for GRID B, the current variation is smaller in the case of greater short circuit power.

Figure 20 describes the variations in voltage and frequency on the PCC of the two grids. It is shown that the stronger grid has less significant variations in both voltage and frequency in the PCC. The voltage and frequency have the same variation according to the power changing in each grid.
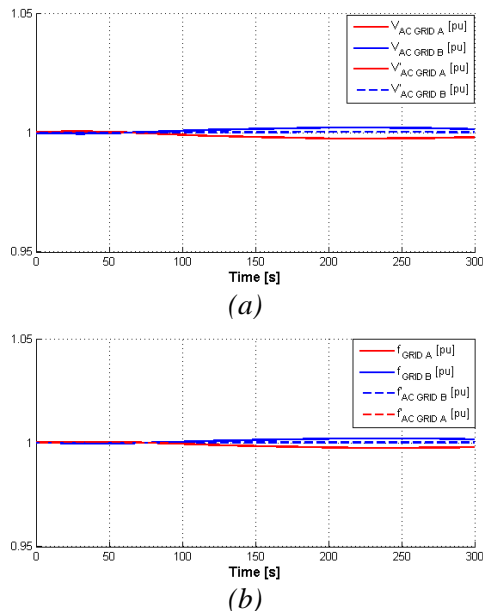

(a)

(b)

Fig. 20. *Voltage (a) and frequency (b) on the busbar of GRID A and GRID B*

4.4. Study Case 4 - Reactive Power Control at the Receiving End Stations

The TSO of each grid is responsible for the control of the reactive power. This control is made independently from one converter to another and also from the WF controller.

Limitations are applied to the operating conditions in reactive power regulation due to the VSC operation parameters. Based on [5] the limits of the reactive power consumption and generators are considered to be between -0.5 and 0.5 pu, where the base value is the active power. Simulation conditions: the output power of the wind farm is constant and the active power regulation for GRID A and GRID B follows the curves from Figure 21.
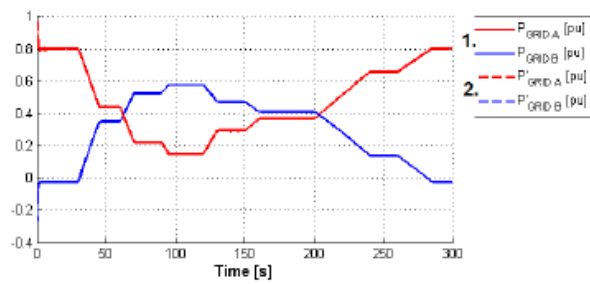

Fig. 21. *Active power sharing between GRID A and GRID B in Case 1 and Case 2*

During the simulation time different values for reactive power demand were chosen, as shown in Figure 22. Q_{TSOA} and Q_{TSOB} represent the TSO's references for reactive power. A positive value of reactive power indicates reactive power generation into the PCC while a negative value corresponds to reactive power consumption from the grid. Figure 22 demonstrates that the reactive power obtained in the PCC of each grid follows the TSO requirements and that is limited by the operation points of the converters. The TSO has to demand reactive power in the interval [-0:5; +0:5]. In the simulation it was supposed that the grid operator of the GRID B sends the command for 0.7 pu. It can be seen that the inverter manage to limit the reactive power to the minimum limit of -0.5 pu.
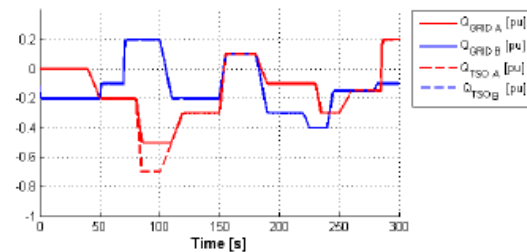

Fig. 22. *Reactive power regulation in the GRID A and GRID B PCC*

The reactive power flow is the result of changing the voltage amplitude by means of the phase reactors. If the voltage on the grid side is greater than the voltage on the converter side it will result reactive power consumption mode, otherwise the converter will generate reactive power. The next two figures illustrate the relation between the reactive power and the voltage levels in the PCC and at the AC terminal of the converters.

The AC voltage from the converters follows the variations of the reactive power in Figure 23. The simulation results of the voltages in the PCCs of the grids are presented in Figure 24 and show small variations comparing to the converters AC voltages.
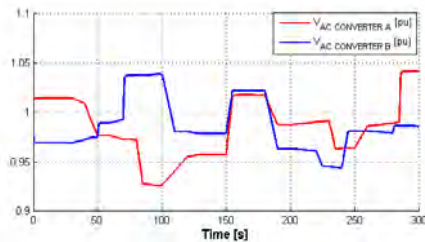
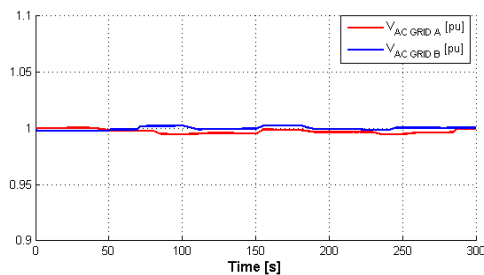***Fig. 23.*** *AC voltage fluctuations at CONVERTER A and CONVERTER B*

Fig. 24. *Voltage variations in the GRID A and GRID B PCC*

The simulation results conclude that the objectives of the reactive power controller have been accomplished. The main goal was to control independently the reactive power for each grid. The reactive power regulation was performed in real time according to the TSOs request and it complies with the nominal operation of the converter. For a more precise control, the active power through the converter has to be considered and the reactive power control should follow the typical PQ diagram for VSC.

5. Conclusions

The perspective of DC power interchange between three or more terminals has been under active consideration for the last years. This paper presents a proposed three terminal VSC-HVDC model linking two onshore grids and one offshore wind farm. The main focus was on developing the control strategy for connecting these three systems via DC connection. A significant interest was shown not only for the modelling and implementation of the transmission system, the converters and their control, but also on the development of the WF components and their control. All the models have been designed and build in DIgSILENT Power Factory. The major achievement is the assessment of the control method for the 'Multiterminal DC Connection'. This proved to be a feasible solution and could be the solution for futures projects regarding the algorithm, extending it to 'n' number of systems, this might be the answer for the 'Supergrid' project connection of large offshore wind farms with far distances from the land. By improving the control

References

[1]. **European Wind Energy Association**. *Wind Energy - The Facts.* [cited 5 March 2009]. Available from:ww.ewea.org/leadmin/ewea_documents/documents/publications/WETF/1565_ExSum_ENG.pdf

[2]. **Ervin Spahi̧c and Gerd Balzer**. *Offshore Wind Farms* - VSC-based HVDC Connection. Power Tech, 2005 IEEE Russia. ISBN: 978-5-93208-034-4

[3]. **Adelina Agap and Cristina Madalina Dragan** - *Multiterminal DC Connection for Offshore Wind Farm.* Master thesis, Institute of Energy Technology, Aalborg University. Aalborg 2009.

[4]. **Florin Iov** - *VSC based DC Transmission System for connecting Active Stall Wind Farms to Grid* . Risø Library. Aalborg University 2004.

[5]. **Adelina Agap, Adrian Constantin, Cristina Madalina Dragan and Borja Imanol Markinez Iurre** - Modelling, *Operation and Control of HVDC* Connected Oshore Wind Farms. Third semester project at Institute of Energy Technology. AAU, 2008.

[6]. **S. Douangsyla, P. Indarack, A. Kanthee, M. Kando, S. Kittiratsatcha and V. Kinnares** - *Modelling for PWM Voltage Source Converter Controlled Power Transfer*, 2004. International Symposium on Communications and Information Technologies. Sapporo, Japan.

[7]. **Temesgen M. Haileselassie, Marta Molinas** - *Tore Undeland. Multiterminal VSC-HVDC* System for Integration of Oshore Wind Farms and Green Electrication of Platforms in the North Sea. NORPIE/2008, Nordic Workshop on Power and Industrial Electronics, June 9-11, 2008.

[8]. **ABB** - *It's time to Connect.* Technical description of HVDC Light® technology. ABB - Grid Systems - HVDC. SE-771 80 Ludvika, Sweden.

[9]. **Power Factory** - *DIgSILENT G*mbh. PWM Converter - Technical Reference.Power Factory v. 3.2 - Help Manual.

[10]. **B. Burger, A. Engel** - Fast Signal Conditioning in Single Phase Systems. Institut fürSolare Energieversorgungstechnik (ISET) e. V. EPE 2001.